Eur. Phys. J. D (2017) 71: 46
DOI: 10.1140/epjd/e2017-70405-7

THE EUROPEAN PHYSICAL JOURNAL D

Regular Article

Production of the Q_2 doubly excited states of the hydrogen molecule by electron impact in a single step

Leonardo O. Santos[1,a], Alexandre B. Rocha[2], Nelson Velho de Castro Faria[1], and Ginette Jalbert[1]

[1] Instituto de Física, Universidade Federal do Rio de Janeiro, Cx. Postal 68528, 21941-972 Rio de Janeiro, Brazil
[2] Instituto de Qumica, Universidade Federal do Rio de Janeiro, 21941-909 Rio de Janeiro, Brazil

Received 23 June 2016 / Received in final form 24 September 2016
Published online 2 March 2017 – © EDP Sciences, Società Italiana di Fisica, Springer-Verlag 2017

Abstract. We calculate the single step cross sections for excitation of Q_2 states of H_2 and its subsequent dissociation. The cross section calculations were performed within the first Born approximation and the electronic wave functions were obtained via State-Averaged Multiconfigurational Self-Consistent Field followed by Configuration Interaction. We have assumed autoionization is the only important process competing with dissociation into neutral atoms. We have estimated its probability through a semi classical approach and compared with results of literature. Special attention was given to the $Q_2\ ^1\Sigma_g^+(1)$ state which, as has been shown in a previous work, may dissociate into $H(2s\sigma)$ + $H(2s\sigma)$ fragments (some figures in this article are in colour only in the electronic version).

1 Introduction

Doubly excited states of the H_2 molecule play an important role in collisional process such as electron impact excitation [1], associative ionization [2] and $e^- + H_2^+$ scattering [2–5]. These states are so-called because its two electrons occupy excited orbitals, lying above the molecular orbital $1s\sigma_g$. As a direct consequence, the states are localized above the ionization threshold of H_2^+. Such states are also known as Q_n states because they are closely related to the Feshbach formalism [6]. The Q_n states may autoionize yielding to $H_2^+ + e^-$, $H + H^+ + e^-$ or dissociate into H^+ + H^- ions as well as into neutral excited H atoms that would be a possible route towards entangled atom pairs.

Many experimental investigations have been devoted to the analysis of the different ionic and/or neutral fragments. For example, in 1973 Browning and Fryar [7] measured the ratio between dissociative and non-dissociative ionization (H^+/H_2^+) arising from photo absorption. They found an increase of that ratio near 26 eV due to the presence of doubly excited states.

The first theoretical calculations related to doubly excited states were carried out by Bottcher and Docken in 1974 [8], who calculated the energies and widths for dissociative states $Q_1\ ^1\Pi_u$ and $Q_2\ ^1\Pi_u$ in the internuclear range of 1 a.u. $\leq R \leq$ 10 a.u. Guberman, in 1983 [9] calculated 24 doubly excited states using the Configuration Interaction (CI) [10] within the Feshbach projection operators formalism [6] and has been an important reference for many years. It is worth mentioning the work of Tennyson and Noble [11] who calculated the positions and widths of all the low-lying Σ and Π resonances in the electron-H_2^+ collision as functions of internuclear distance by using R-matrix method. Nikitin et al. [12] in the context of cold collisions investigated the interaction between two excited hydrogen atoms, obtaining asymptotics doubly excited states at the great distances. In the same context, Forrey et al. [13,14] obtained cross sections and yield rates of metastable hydrogen atoms including Lamb shift and fine structure in their calculations. In the late 90's, Sánchez and Martín [15] calculated dozens of potential energy curves and autoionization widths of Q_2 doubly excited states using the Feshbach projection operators formalism and wavefunctions with one-center B-spline expantion. In 2002, Jonsell et al. [16] used explicitly correlated basis functions and complex-scaling method for potential energy curves and autoionization width calculations, respectively. Vanne et al. [17] calculated the doubly excited H_2 states converging to $H(2l)$ + $H(2l')$ using B-spline basis functions with prolate spheroidal coordinate system (two-center expansion).

From the experimental point of view, most of the works in photoabsorption are related to dissociation by single photon impact and due to the selection rule which applies in such cases, only states with certain symmetries ($^1\Sigma_u^+$ and $^1\Pi_u$, for example) are accessed. For example, Bosek et al. [18] measured the cross sections for the formation of the metastable atomic hydrogen in the $2s$ state in photoexcitation of H_2 and D_2 as a function of the incident photon energy in the range of the doubly excited states. Optically forbidden states has also been investigated through resonance-enhanced multiphoton ionization (REMPI) technique [19,20] that is more efficient to access

[a] e-mail: leonardosantos@if.ufrj.br

a specific state. With regard to collisions by electron impact, in which states of symmetry $^1\Sigma_g^+$ are accessible (as well as in REMPI), few works [21,22] have been conducted as, for example, Ishikawa et al. [21] who measured differential cross sections of the dissociative double excitations resulting in H($2p$) in 80 eV electron collisions with H_2 by means of angle-resolved electron energy loss spectroscopy in coincidence with detecting Lyman-α photons. No group, except ours, has reported the detection of H($2s$) + H($2s$) coincident fragments [23].

We have previously investigated the optically forbidden transition from ground to $Q_2\ ^1\Sigma_g^+$ state that may dissociate into H($2s$) + H($2s$) metastable fragments [24] and, as we said, experimental data confirm its existence [23]. Now, we present our calculated excitation cross sections from ground to the repulsive doubly excited states $Q_2\ ^1\Sigma_g^+(1)$, $Q_2\ ^1\Sigma_g^+(2)$, $Q_2\ ^1\Sigma_g^+(3)$, $Q_2\ ^1\Sigma_u^+(1)$, $Q_2\ ^1\Pi_u(1)$, $Q_2\ ^1\Pi_u(2)$ and $Q_2\ ^1\Pi_g(1)$ within the first Born approximation (FBA). Ground and excited state wavefunctions were obtained at the Configuration Interaction level from State Averaged Multiconfigurational Self Consistent Field molecular orbitals in which states with the same symmetry as the ground state were optimized.

In order to compute dissociation from excitation cross sections, we have used the resonance widths of Fernandez and Martín [25] and a semiclassical approximation [26] in order to estimate the survival factor χ_d, for $Q_2\ ^1\Sigma_g^+(1)$, $Q_2\ ^1\Sigma_g^+(2)$, $Q_2\ ^1\Sigma_g^+(3)$, $Q_2\ ^1\Sigma_u^+(1)$ and $Q_2\ ^1\Pi_u(1)$ (the numbers in brackets represent the order of the root with a given symmetry) states. Then, combining the survival factor and the calculated CI excited cross sections, we obtained the dissociation cross sections for production of H($2l$) + H($2l'$) through these states. This results can be very helpful for future experimental investigations of those states, which lead to dissociation into two hydrogen atoms at $2s$ state.

2 Theoretical background

2.1 Excitation and dissociation cross-sections

Calculations were performed within the first Born approximation (FBA) for incident electron energies in the range 100 eV–800 eV. FBA is certainly valid in the upper limit of this range and furnishes a good estimation in the lower part. The inclusion of 100 eV as lower limit in the present study is motivated by a previous work of our group on twin atoms [23], where we used electrons with energies ranging in the interval 60 eV–200 eV. We are interested in a collisional process in which a H_2 molecule, initially in the ground vibro-electronic state, is excited by a 100 eV electronic projectile to the purely repulsive Q_2 states.

As said before, when the doubly excited states are accessed, two main channels are in competition: the H_2 molecule may dissociate into excited neutral fragments or autoionize. In particular, the aim of this paper is to shed light to the dissociative channels that yield excited neutral metastable non radiative H($2s$) fragments which has a life-time sufficient to go through a longitudinal Stern-Gerlach atomic interferometer [27] without decay. In the FBA approach, the double differential excitation cross section (DDECS) of excitation to these dissociative Q_n states is given by [28]

$$\frac{d^2\sigma_{0n}}{d\omega dE} = (2\pi)^2 \frac{1}{2K^2}\frac{k_n}{k_0}\frac{1}{E}\frac{df_{0n}(K,E)}{dE} \tag{1}$$

where $\omega = (\theta, \phi)$ stands for the solid angle of the scattered projectile measured from the electron beam, k_0 and k_n it initial and final momentum respectively, E is the transition energy and K, the transferred momentum to the target. The scattering angle and the transferred momentum are directly related through $d\omega = 2\pi sen\theta d\theta = 2\pi K dK/k_0 k_n$.

For a molecular system,

$$\frac{df_{0n}(K,E)}{dE} = \frac{2E}{K^2}\frac{g_n}{4\pi}|\epsilon_{0n}(K;\nu,M,J \leftarrow \nu_0,M_0,J_0)|^2 \tag{2}$$

where g_n is the degeneracy of the final electronic state (two for a Π_u state) and

$$\epsilon_{0n}(K;\nu,M,J \leftarrow \nu_0,M_0,J_0) = \langle \Psi_n | \sum_{i=1}^{2} \exp(i\mathbf{K}.\mathbf{r}_i) | \Psi_0 \rangle \tag{3}$$

is the so called *form factor* for the transition between the molecular ground state and an excited state.

In order to obtain single differential cross sections as a function of transition energy, i.e.

$$\frac{d\sigma_{0n}}{dE} = \int \left(\frac{d^2\sigma_{0n}}{d\omega dE}\right) d\omega \tag{4}$$

we change the variable of integration to the more convenient $d\ln K^2$ and equation (1) becomes:

$$\frac{d\sigma_{0n}}{dE} = (\pi^2)\frac{1}{E_{imp}}\int \frac{1}{E}\frac{df_{0n}(K,E)}{dE} d\left(lnK^2\right) \tag{5}$$

where $E_{imp} = k_0^2/2$ stands for the energy impact of the projectile.

The molecular wavefunctions $\Psi_0(r_1, r_2; \mathbf{R})$ and $\Psi_n(r_1, r_2; \mathbf{R})$, calculated within the Born-Oppenheimer approximation [29] will be explained in next section.

The processes we are interested in, the dissociation into two neutral excited atoms, are in competition with autoionization. Neglecting other effects like non-adiabatic coupling, dissociation cross section σ_{diss}, can be estimated through the expression

$$\sigma_{diss} = \chi_d \sigma_{0n} \tag{6}$$

where χ_d is the survival factor of the final state. It can be calculated within a semiclassical approach [26,30]

$$\chi_d(E, R_0) = \exp\left(-\int_{R_0}^{R_x} \frac{\Gamma(R)}{v(R)} dR\right) \tag{7}$$

where $\Gamma(R)$ is the theoretical autoionization width obtained by Sánchez and Martín [31].

The low integration limit $R_0 = 1.2$ a.u. corresponds to the left border of the Franck-Condon region for the H_2 molecule, and R_x, the stabilization point, was chosen by the very same criteria as in previous works [30,32], i.e., we have used the last calculated points for R_x for Q_2 states, since there is no crossing between levels which leads to the ground state. The quantity $v(R)$ in equation (7) is the semiclassical radial velocity of the two nuclei [26]

$$v(R)=\frac{1}{\mu^{1/2}}\left[(E-V(R))\left((E-V(R))^2\left(\frac{\Gamma(R)}{2}\right)^2\right)^{1/2}\right]^{1/2}. \quad (8)$$

2.2 Target wavefuncion

Within the Born-Oppenheimer approach the molecular wavefunction is given by:

$$\Psi_0(r_1,r_2;\mathbf{R}) = Y_{J_0M_0}(\Theta,\Phi)\chi_{0J_0}(R)\psi_0(\mathbf{r_1},\mathbf{r_2};\mathbf{R})$$
$$\Psi_n(r_1,r_2;\mathbf{R}) = Y_{JM}(\Theta,\Phi)\chi_{nW}(R)\psi_n(\mathbf{r_1},\mathbf{r_2};\mathbf{R}) \quad (9)$$

where r_1 and r_2 stands for the electronic coordinate and R is the internuclear distance. The spherical harmonics $Y_{J_0M_0}(\Theta,\Phi)$ and $Y_{JM}(\Theta,\Phi)$ are the rigid rotor eigenfunctions for initial and final rotational states, respectively; χ_{0J_0} is the discrete vibrational wavefunction and χ_{nW} the continuum one and finally ψ_0 and ψ_n stands for, respectively, the initial and final electronic wavefunctions.

The ground and vibrational continuum wavefunctions and their eigenvalues were obtained by integrating numerically the Schroedinger equation for the nuclei making use of Le Roy et al.'s routines [33], in which we have used our own potential energy curves [24] for the ground and vibrational continuum states.

The doubly excited electronic states were obtained by using the package GAMESS [34,35] which, among other features, calculates the non-relativistic electronic energy of the ground and excited electronic states of molecules within the Born-Oppenheimer approximation [29]. The electronic states were described by an ab initio wavefunction constructed within the Huzinaga's [36] basis set of Cartesian Gaussian-Type $(12s,6p,3d,1f)/[9s,6p,3d,1f]$ orbitals in which the full space consisted of 110 orbitals of which $29\sigma_g$, $29\sigma_u$, $22\pi_g$, $22\pi_u$, $2\delta_g$, $2\delta_u$, $2\phi_g$ and $2\phi_u$ was used. Within this space, we have used the State Averaged Multiconfigurational Self Consistent Field (SA-MCSCF) [37], followed by Configuration Interaction (CI) [10].

In the SA-MCSCF step, the configurations were generated within the point group C_{2v}, which is a subgroup of the actual H_2 group, i.e., $D_{\infty h}$, and all states that belonged to the same irreducible symmetry, $^1\Sigma^+$, were optimized with equal weight. The reduction of the point group from $D_{\infty h}$ to C_{2v} was done in order to allow states of different irreducible representation in the original group to lie in the same irreducible representation in the subgroup (σ_g and σ_u) $\rightarrow \sigma$. This procedure allows states Σ_g and Σ_u to be optimized on the same footing. The active space was consisted of 12 molecular orbitals of which: $n\sigma_g$ ($n = 1$–4), $n\sigma_u$ ($n = 1$–4), $n\pi_g$ ($n = 1$–2), $n\pi_u$ ($n = 1$–2).

Thus, it was optimized both $\mathcal{P} = |1\sigma_g\rangle\langle 1\sigma_g| + |1\sigma_u\rangle\langle 1\sigma_u|$ and $\mathcal{Q} = 1 - \mathcal{P}$ spaces. It is desirable to have an accurate set of $\mathcal{P}$-space configurations in order to describe continuum wavefunctions in the future. In the CI approach, we have used a larger active space. It should be mentioned the doubly excited states lie at a high root in the CI matrix eigenvalue approach which, in general, is arduous to converge. Thus, in order to eliminate from calculation some spurious states and obtain converged matrix elements between so distant states, i.e., ground and doubly excited, we have used 20 of 110 available molecular orbitals of which 12 previously optimized via SA-MCSCF.

2.3 Form factor

Excitation cross-sections were performed within the Q-branch and rotational average approaches regarding the rotational motion and the fixed nuclei approximation for the electronic transition that was performed at $R = R_{eq}$, i.e., the equilibrium geometry of the molecular target.

The Q-branch approach was performed through the transitions $J = 0 \rightarrow J' = 0$ and $J = 1 \rightarrow J' = 1$. Remembering that the rotational wavefunctions are given by:

$$\mathcal{Y}_{JM}(\Theta,\Phi) = N_J^M e^{iM\Phi} P_J^{|M|}(\cos\Theta) \quad (10)$$

where

$$N_J^M = \sqrt{\frac{(2J+1)(J-|M|)!}{4\pi(J+|M|)!}}. \quad (11)$$

For $J = 0, 1$ and $M = 0$, one gets:

$$\mathcal{Y}_{00}(\Theta,\Phi) = \sqrt{\frac{1}{4\pi}}$$
$$\mathcal{Y}_{10}(\Theta,\Phi) = \sqrt{\frac{3}{4\pi}}\cos(\Theta). \quad (12)$$

The expressions for the form factor in the Q-branch approach (Eq. (3)) became for $J = 0 \rightarrow J' = 0$

$$|\epsilon_{0n}(K;\nu,0,0\leftarrow 0,0,0)|^2 = \frac{q_{00}}{16\pi^2}\left|\int \epsilon'_{0n}(K,R_{eq},\Omega)d\Omega\right|^2 \quad (13)$$

and for $J = 1 \rightarrow J' = 1$

$$|\epsilon_{0n}(K;\nu,0,1\leftarrow 0,0,1)|^2 = \frac{9q_{11}}{16\pi^2}\left|\int \epsilon'_{0n}(K,R_{eq},\Omega)cos\Theta d\Omega\right|^2 \quad (14)$$

where:

$$q_{JJ'} = \left|\int dR\chi^*_{EJ'}(R)\chi_{0J}(R)\right|^2 \quad (15)$$

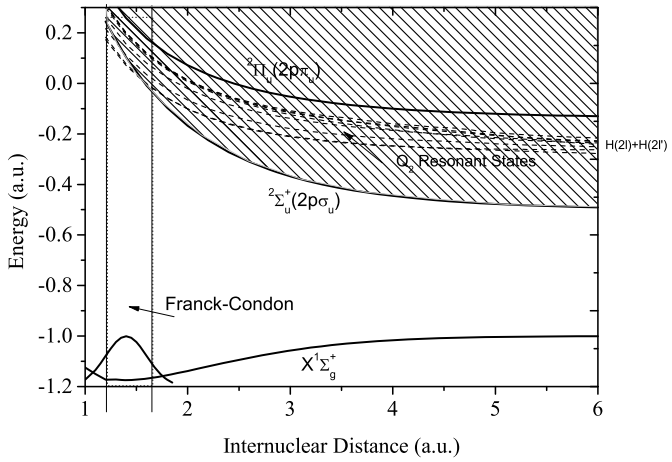

Fig. 1. Process involving the excitation from the ground electronic to the dissociative Q_2 states converging into H($2l$) + H($2l'$) neutral fragments for some symmetries; the shaded region represents the continuum of the molecule.

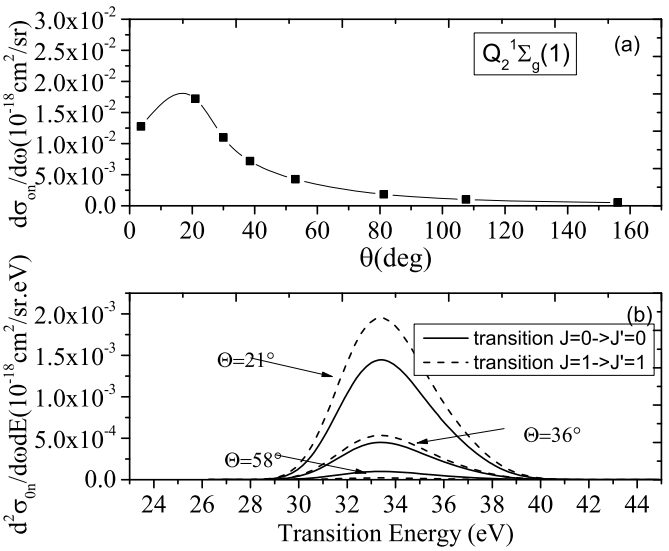

Fig. 2. (a) Single differential cross section obtained from equations (1) (integrated over the transition energy) and (13) for the state $Q_2\ ^1\Sigma_g^+(1)$ as a function of the scattering angle; (b) double differential excitation cross section (DDECS) for the state $Q_2\ ^1\Sigma_g^+(1)$ as a function of transition energy for some scattering angles; all calculations in the Q-branch approach and at energy impact $E_{imp} = 100$ eV.

is the Franck-Condon factor and $\epsilon'_{0n}(K, R_{eq}, \Omega)$ the *electronic form factor* at $R = R_{eq}$.

In this work we have only considered the $M_J = 0$ case because the collisional process under investigation is invariant under a Φ rotation.

We now consider the rotational average approach. It is an useful theoretical tool, mainly when electron impact experiments are to be compared to, since in such cases one can consider the rotational states of molecule as effectively degenerate by summing over all states J, M and then, making an average on J_0, M_0 [28]. Thus, the form factor of equation (3) becomes:

$$|\epsilon_{0n}(K;\nu \leftarrow 0)|^2 = \frac{q_{JJ'}}{4\pi}\int d\Omega\,|\epsilon'_{0n}(K, R_{eq}, \Omega)|^2\,. \quad (16)$$

In the next section we present our calculations for excitation cross-sections in both approaches and results are discussed.

3 Results and discussion

Figure 1 shows the excitation by electron impact to Q_2 series of doubly excited states that can, if they survive, dissociate into neutral fragments in which at least one of them is excited. We note that, in the Franck-Condon region, the Q_2 states of lower energy cross the $^2\Sigma_u^+$ curve which may influence their probability of surviving in the dissociative limit.

3.1 Q-branch

In many experiments of electron-molecule collision, it is not possible to define precisely the rotational quantum number of the initial state, which implies that rotational contribution should be taken as an average over possible states. However, when temperature is low, only the lowest rotational levels are populated. Besides, electron impact collisions are not likely to cause rotational excitations on the molecule. Therefore, the Q-branch transitions can be assumed to be a good approximation for such systems. Figure 2a presents the single differential excitation cross section for the Q-branch transition $J = 0 \rightarrow J' = 0$ as a function of the scattering angle for the state $Q_2\ ^1\Sigma_g^+(1)$ (the first root) and for an impact energy of 100 eV. It was calculated from equations (1) and (13) and for scattering angles in the range $\theta_{min} \approx 0 \leq \theta \leq \theta_{max} \approx 173$. This figure shows a maximum around 20 degree. There is no benchmark to compare with, but it can be observed that the curve behaves like an ordinary optically forbidden transition. Figure 2b presents the double differential excitation cross sections (DDECS) as a function of the transition energy (see Eq. (1)) and for several scattering angles $\theta = 21$, 36 and 58 and for the Q-branch $J = 0 \rightarrow J' = 0$ and $J = 1 \rightarrow J' = 1$ transitions obtained from equations (13) and (14). Maxima around 33 eV can be observed for several scattering angles. We can also observe that the $J = 1 \rightarrow J' = 1$ transitions are more likely to happen for smaller scattering angles than the $J = 0 \rightarrow J' = 0$ ones which have higher contribution for $\theta \geq 58$.

3.2 Rotational average

We present in Figure 3 the calculated cross sections as a function of the transition energy E for several states that may dissociate into excited neutral fragments H($2l$) + H($2l'$); the cross sections were obtained from equations (1) and (16) for an energy impact of 100 eV.

The limits of the K integration (see Eq. (5)), i.e., K_{min} and K_{max} were obtained in the same way that Cann

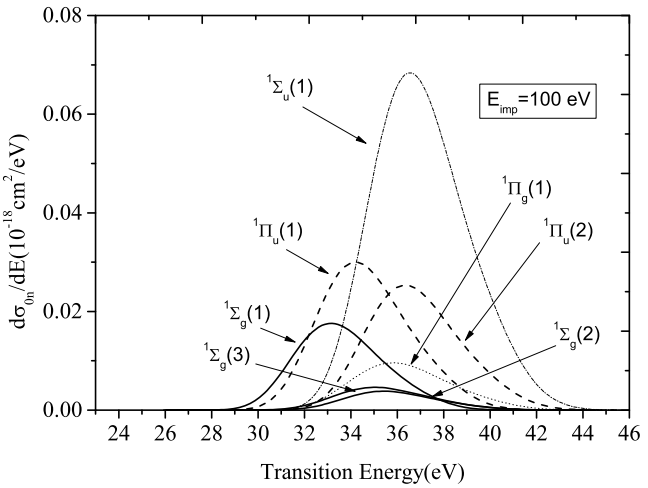

Fig. 3. Differential excitation cross sections for some Q_2 states as a function of transition energy (rotational average calculated from Eq. (15)): number in brackets stands for the order of the root in CI eigenvalue approach.

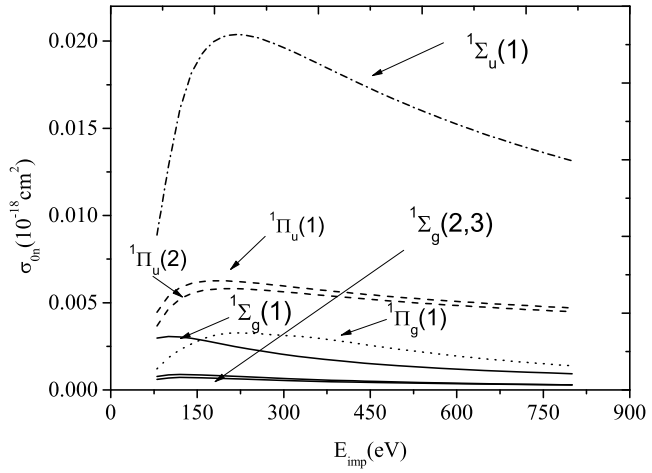

Fig. 4. Total cross section of excitation to Q_2 states (obtained from an average rotational calculation see Eq. (15)) as a function of the energy impact.

and Thakkar [39]. The cross sections present maxima between 33 and 37 eV which is approximately the energy range of Q_2 states calculated from the ground state. Note that all optically forbidden states ($^1\Sigma_g^+$,$^1\,\Pi_g$) have lower cross sections than the allowed ones ($^1\Sigma_u^+$,$^1\,\Pi_u$). The explanation is that the major contributions to the excitation cross section come from collisions with low transferred momentum which is close to the optical regime.

Figure 4 shows the total excitation cross section as a function of the impact energy of the electron. In order to obtain it, we have integrated equation (1) considering the adequate limits of integration K_{min} and K_{max} for each energy impact and then integrated in the transition energy variable. We observed that the allowed transitions present higher cross sections than the forbidden ones. Also, a maximum is found for the $^1\Sigma_g^+(1,2,3)$ states for impact energy smaller than 150 eV, the $^1\Pi_u(1,2)$ present maxima around 150 eV, $^1\Sigma_u^+(1)$ has a maximum around 200 eV as well as $^1\Pi_g(1)$.

3.3 Dissociation

We consider that only two processes may occur along the dissociative dynamics of the excited states: autoionization or dissociation in neutral fragments H($2l$) + H($2l'$). Thus, the dissociation cross sections are related to the excitation cross sections through the survival factors χ_d which are shown in Table 1.

We have calculated χ_d within a semiclassical approach [26], in which we have used the autoionization width $\Gamma(R)$ from Fernández and Martín [25] and the nuclear velocity v(R) from our own potential energy curves (see Eq. (8)). In Table 1 the present results are compared with other theoretical [32] and experimental [40] survival factors. Discrepancies between the experimental values and the theoretical ones are observed although the theoretical ones have a good agreement with each other.

Table 1. Theoretical [32] and experimental [40] estimated survival factors.

	$\chi_d(E)$ present	$\chi_d(E)$ [32]	$\chi_d(E)$ [40]
$Q_1\ ^1\Sigma_u^+(2)$	0.81	0.85	0.50
$Q_1\ ^1\Pi_u(1)$	0.90	0.91	0.26
$Q_2\ ^1\Sigma_g^+(1)$	0.58	0.61	
$Q_2\ ^1\Sigma_g^+(2)$	0.74		
$Q_2\ ^1\Sigma_g^+(3)$	0.68		
$Q_2\ ^1\Sigma_u^+(1)$	0.70		
$Q_2\ ^1\Pi_u(1)$	0.71	0.65	0.10
$Q_3\ ^1\Pi_u(1)$	0.02		
$Q_3\ ^1\Pi_u(2)$	0.03		

These can be due to the numerical integration performed in equation (7), specifically the R_0 and R_x values which are determined by two criteria: an intersection with the ionic potential curve or up to the highest value of R_x for which there is a value for $\Gamma(R)$ calculated. Further, in the experimental case a state that coupled to another can be recorded as autoionized, interfering with the experimental value of χ_d.

Figure 5 shows the results for the dissociation of the states obtained from equation (5) as a function of the Kinetic Energy Released (KER) of their fragments. The kinetic energy released is approximately the kinetic energy relative to the laboratory framework, i.e., $KER = (E(R) - E(\infty))/2$, with half of the total internal energy released for each fragment. Excitation cross sections from which dissociation was obtained, were calculated from the rotational average approach.

At this point, we should emphasize that the neglected non-adiabatic interactions could be responsible for discrepancies in the cross-sections values. Some estimative of the discrepancy due this point was considered by Glass-Maujean and Schmoranzer [40] who estimated the population of the dissociation channel H($2p\pi$) + H($2p\sigma$) as being 82% due to the $Q_2\ ^1\Pi_u(2)$ and 18% as a mix of $Q_1\ ^1\Pi_u(1)$ and $Q_2\ ^1\Pi_u(1)$ states.

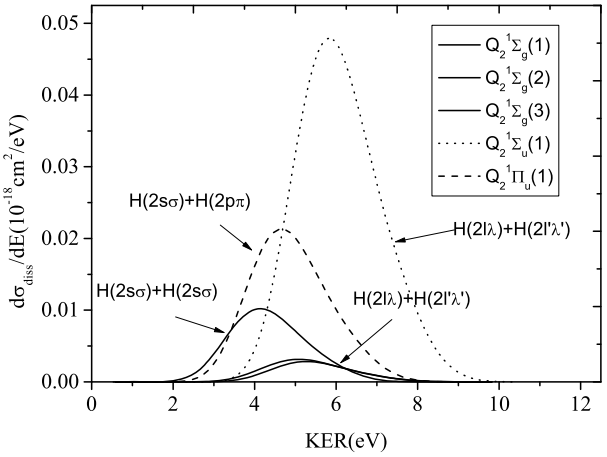

Fig. 5. Dissociation in neutral H($2l$) + H($2l'$) fragments cross section as a function of the kinetic energy released.

According to Glass-Maujean and Schmoranzer [40], who worked with states acessible by impact of photons, the Q_2 $^1\Pi_u(1)$ and $^1\Pi_u(2)$ states dissociate adiabatically into excited neutral fragments H($2s\sigma$) + H($2p\pi$) and H(2pπ) + H(2pσ) respectively, and are in part responsible for the fast peaks H($2s$). Taking advantage of the MR-CI method used in this paper, we can conclude that the state Q_2 $^1\Sigma_g^+(1)$ dissociates adiabatically into H($2s\sigma$) + H($2s\sigma$) [24]. The Q_2 $^1\Sigma_u^+(1)$, $^1\Sigma_g^+(2)$ and $^1\Sigma_g^+(3)$ states have unknown dissociative limits and they were indicated by the usual notation H($2l\lambda$) + H($2l'\lambda'$), where l stands for angular momentum in separated atom limit and λ, for the projection of the MO angular momentum along the nuclear axis.

From the Figure 5 we can assert the energy position of the peaks of these fragments that lie in the range of about 4 eV to 6 eV in agreement with our previous theoretical work and experimental data [41].

4 Conclusions

This work presents theoretical investigations on Q_2 doubly excited states of H_2 molecule promoted by electron impact. The scattering process is described within the first Born approximation. Electronic wave functions were obtained at MCSCF/CI level.

For Q-branch ($J = 0 \rightarrow J' = 0$), the double differential excitation cross section (DDECS) for the transition from ground to Q_2 $^1\Sigma_g^+(1)$ state as a function of scattering angle, for a impact energy of 100 eV, shows a maximum around 20 degree and a profile of forbidden transition. The DDECS for ($J = 0 \rightarrow J' = 0$) and ($J = 1 \rightarrow J' = 1$) transitions are also plotted against transition energy, maxima are found around 33 eV for several scattering angles and dependence on scattering angle of dominant transition is found. When rotationally averaged, the maximum does not shift significantly. In this case, DDECS for Q_2 $^1\Sigma_g^+(1)$ has the same order of magnitude of other allowed and forbidden transitions from ground to Q_2 states, the allowed lying above, which means that the main contribution comes from low transferred momentum.

When dissociation cross section is plotted against kinetic energy released of the fragments, a maximum is found around 4 eV for the Q_2 $^1\Sigma_g^+(1)$ state and lies in the 4–6 eV range for all Q_2 states considered. Total cross sections were also obtained for all the Q_2 states and we found its maxima around 150–200 eV.

Authors contribution statement

All authors contributed equally to the accomplishment of this work.

This work is supported by CAPES, FAPERJ and CNPq.

Appendix

A.1 Rotational averaging

In this appendix we show how the rotational averaging is performed.

First of all, one should remember that:

$$\sum_{J=0}^{\infty}\sum_{M=-J}^{J}\mathcal{Y}^*_{JM}(\Omega)\mathcal{Y}_{JM}(\Omega') = \delta(\Omega-\Omega') \tag{A.1}$$

where $\mathcal{Y}_{J,M}(\Theta,\Phi)$ are the spherical harmonics and $\Omega = (\Theta,\Phi)$ the angles between the internuclear axis and the momentum transfer vector.

Let's consider $F(\Omega)$ as a smooth and monotonic function of the variables Θ and Φ. We are going to show that:

$$\sum_{J,M}\left|\int \mathcal{Y}^*_{JM}(\Omega)F(\Omega)\mathcal{Y}_{JM}(\Omega)d\Omega\right|^2 = \int |F(\Omega)|^2\,|\mathcal{Y}(\Omega)|^2\,d\Omega. \tag{A.2}$$

First, we expand the square module of the left hand side of equation (A.2)

$$\begin{aligned}\sum_{J=0}^{\infty}\sum_{M=-J}^{J}&\int \mathcal{Y}^*_{JM}(\Omega')F(\Omega')\mathcal{Y}_{JM}(\Omega')d\Omega'\\ &\times\int \mathcal{Y}_{JM}(\Omega)F^*(\Omega)\mathcal{Y}^*_{JM}(\Omega)d\Omega\\ &=\int d\Omega'\int d\Omega\sum_{J,M}\mathcal{Y}^*_{J,M}(\Omega')\mathcal{Y}_{J,M}(\Omega)\\ &\times F(\Omega')F^*(\Omega)\mathcal{Y}_{J,M}(\Omega')\mathcal{Y}^*_{J,M}(\Omega).\end{aligned} \tag{A.3}$$

Inserting equation (A.1) into equation (A.3)

$$\begin{aligned}\int d\Omega'\int d\Omega\delta(\Omega-\Omega')&F(\Omega')F^*(\Omega)\mathcal{Y}^*_{J,M}(\Omega)\mathcal{Y}_{J,M}(\Omega')\\ &=\int d\Omega F(\Omega)F^*(\Omega)\mathcal{Y}^*_{J,M}(\Omega)\mathcal{Y}_{J,M}(\Omega)\\ &=\int d\Omega\,|F(\Omega)|^2\,|\mathcal{Y}_{J,M}(\Omega)|^2.\end{aligned} \tag{A.4}$$

This demonstrates equation (A.2).

Before proceeds, few comments have to done:

1. the J dependence in the electronic transition matrix is not only through spherical harmonics but also due vibrational wavefunction $\chi_{E,J}(R)$. However we have assumed that the J dependence on vibrational wavefunction can be approximated by a certain $J \to \tilde{J}$. It is a good approximation provided the rotational occupancy $J \sim 1$. It is precisely the case of the H_2 molecule at room temperature;
2. in the range 100 eV $< E_{imp} <$ 1000 eV, we are certainly unable to extract any information about the rotational transitions. So we consider the rotational states as effectively degenerates and sum up to ∞.

Thus, the oscillator strength in equation (2) (manuscript) can be written as:

$$\left(\frac{df_{0n}}{dE}\right)^{n,E}_{0,\nu_0 J_0 M_0} = \sum_{J=0}^{\infty}\sum_{M=-J}^{J}\frac{E}{K^2}\Bigg[\int d\Omega' \mathcal{Y}^*_{JM}(\Omega') \times \int dR' \chi^*_{E,J}(R')\left[\epsilon^*_{0n}(K,R',\Omega')\right]\chi_{\nu_0,J_0}(R')\mathcal{Y}_{J_0M_0}(\Omega') \times \int d\Omega \mathcal{Y}^*_{JM}(\Omega)\int dR \chi^*_{E,J}(R) \times \left[\epsilon_{0n}(K,R,\Omega)\right]\chi_{\nu_0,J_0}(R)\mathcal{Y}_{J_0M_0}(\Omega)\Bigg]. \quad (A.5)$$

Rearranging terms and assuming the conditions above:

$$\left(\frac{df_{0n}}{dE}\right)^{n,E}_{0,\nu_0,J_0,M_0} = \frac{E}{K^2}\int d\Omega \times \left|\int dR \chi^*_{E,J}\epsilon_{0n}\chi_{\nu_0,J_0}\right|^2 |\mathcal{Y}_{J_0,M_0}|^2. \quad (A.6)$$

Now, besides the sum of the final J states, we sum up the $(2J+1)$ times degenerate M_0 states.

$$\begin{aligned}\left(\frac{df_{0n}}{dE}\right)^{n,E}_{0,\nu_0} &= \left\langle \left(\frac{df_{0n}}{dE}\right)^{n,E}_{0,\nu_0,J_0,M_0}\right\rangle \\ &= \frac{\sum_{M_0=-J_0}^{J_0}\left(\frac{df_{0n}}{dE}\right)^{n,E}_{0,\nu_0,J_0,M_0}}{\sum_{M_0=-J_0}^{J_0}\langle J_0,M_0|J_0,M_0\rangle} \\ &= \frac{\sum_{M_0=-J_0}^{J_0}\left(\frac{df_{0n}}{dE}\right)^{n,E}_{0,\nu_0,J_0,M_0}}{\sum_{M_0=-J_0}^{J_0}1} \\ &= \frac{\sum_{M_0=-J_0}^{J_0}\left(\frac{df_{0n}}{dE}\right)^{n,E}_{0,\nu_0,J_0,M_0}}{(2J+1)} \end{aligned} \quad (A.7)$$

where

$$\sum_{M_0=-J_0}^{J_0}|\mathcal{Y}_{J_0,M_0}|^2 = \frac{(2J+1)}{4\pi}. \quad (A.8)$$

Finally, equation (A.5) becomes:

$$\left(\frac{df_{0n}}{dE}\right)^{n,E}_{0,\nu_0} = \frac{E}{K^2}\int\frac{d\Omega}{4\pi}\left|\int dR \chi^*_{E,J}(R)\epsilon_{0n}(K,R,\Omega)\chi_{\nu_0,J_0}(R)\right|^2. \quad (A.9)$$

References

1. R.N. Compton, J.N. Bardsley, in *Electron-Molecule Collisions*, edited by I. Shimamura, K. Takayanagi (Plenum, New York, 1984), Chap. 4
2. X. Urbain, A. Giusti-Suzor, D. Fussen, C. Kubach, J. Phys. B **19**, L273 (1986)
3. B.I. Schneider, L.A. Collins, Phys. Rev. A **28**, 166 (1983)
4. K. Nakashima, H. Takagi, H. Nakamura, J. Chem. Phys. **86**, 726 (1987)
5. L.A. Collins, B.I. Schneider, C.J. Noble, C.W. McCurdy, S. Yabushita, Phys. Rev. Lett. **57**, 980 (1986)
6. H. Feshbach, Ann. Phys. NY **5**, 357 (1958)
7. R. Browning, J. Fryar, J. Phys. B **6**, 364 (1973)
8. C. Bottcher, K. Docken, J. Phys. B **7**, L5 (1974)
9. S.L. Guberman, J. Chem. Phys. **78**, 1404 (1983)
10. B.R. Brooks, H.F. Schaefer, J. Chem. Phys. **70**, 5092 (1979)
11. J. Tennyson, C.J. Noble, J. Phys. B **18**, 155 (1985)
12. S.I. Nikitin, V.N. Ostrowskii, N.V. Prudov, Sov. Phys. J. Exp. Theor. Phys. **64**, 745 (1986)
13. R.C. Forrey, S. Jonsell, A. Saenz, P. Froelich, A. Dalgarno, Phys. Rev. A **67**, 040701 (2003)
14. R.C. Forrey, A. Dalgarno, Y.V. Vanne, A. Saenz, P. Froelich, Phys. Rev. A **76**, 052709 (2007)
15. I. Sánchez, F.Martín, J. Chem. Phys. **110**, 6702 (1999)
16. S. Jonsell, A. Saenz, P. Froelich, R.C. Forrey, R. Côté, A. Dalgarno, Phys. Rev. A **65**, 042501 (2002)
17. Y.V. Vanne, A. Saenz, A. Dalgarno, R.C. Forrey, P. Froelich, S. Jonsell, Phys. Rev. A **73**, 062706 (2006)
18. J.D. Bosek, J.E. Furst, T.J. Gay, H. Gould, L.D.A. Kilcoyne, J.R. Machacek, F.Martín, K.W. McLaughlin, J.L. Sanz-Vicario, J. Phys. B **39**, 4871 (2006)
19. C. Cornaggia, D. Normand, J. Morellec, G. Mainfray, C. Manus, Phys. Rev. A **34**, 207 (1986)
20. J.O. Gaardsted, T. Andersen, H.K. Haugen, J.E. Hansen, N. Vaeck, J. Phys. B **24**, 953 (1991)
21. L. Ishikawa, T. Odagiri, K. Yachi, N. Ohno, T. Tsuchida, M. Kitajima, N. Kouchi, J. Phys. B **44**, 065203 (2011)
22. T. Odagiri, N. Uemura, K. Koyama, M. Ukai, N. Kouchi, Y. Hatano, J. Phys. B **28**, L465 (1995)
23. J. Robert, F. Zappa, de C.R. Carvalho, G. Jalbert, R.F. Nascimento, A. Trimeche, O. Dulieu, A. Medina, C. Carvalho, de Castro N.V. Faria, Phys. Rev. Lett. **111**, 183203 (2013)
24. L.O. Santos, A.B. Rocha, R.F. Nascimento, de Castro N.V. Faria, G. Jalbert, J. Phys. B **48**, 185104 (2015)
25. J. Fernández, F.Martín, New J. Phys. **11**, 043020 (2009)
26. W.H. Miller, J. Chem. Phys. **52**, 3563 (1970)
27. A.D. Cronin, J. Schmiedmayer, D.E. Pritchard, Rev. Mod. Phys. **81**, 1051 (2009)
28. M. Inokuti, Rev. Mod. Phys. **43**, 297 (1970)

29. M. Born, J.R. Oppenheimer, Ann. Phys. **389**, 457 (1927)
30. I. Borges Jr., C.E. Bielschowsky, J. Phys. B **33**, 1713 (2000)
31. I. Sánchez, F.Martín, J. Chem. Phys. **106**, 7720 (1997)
32. I. Borges Jr., C.E. Bielschowsky, Chem. Phys. Lett. **342**, 411 (2001)
33. R.J. Le Roy, R.G. Macdonald, G. Burns, J. Chem. Phys. **65**, 1685 (1976)
34. M.S. Gordon, M.W. Schmidt, *Advances in electronic structure theory: GAMESS a decade later*, in *Theory and Applications of Computational Chemistry: the first forty years*, edited by C.E. Dykstra, G. Frenking, K.S. Kim, G.E. Scuseria (Elsevier, Amsterdam, 2005), pp. 1167–1189
35. M.W. Schmidt, K.K. Baldridge, J.A. Boatz, S.T. Elbert, M.S. Gordon,J.H. Jensen, S. Koseki, N. Matsunaga, K.A. Nguyen, S. Su, T.L. Windus, M. Dupuis, J.A. Montgomery, J. Comput. Chem. **14**, 1347 (1993)
36. T.H. Dunning, J. Chem. Phys. **90**, 1007 (1989)
37. H. Nakano, J. Chem. Phys. **99**, 7982 (1993)
38. A.H. Carter, *Classical and Statistical Thermodynamics* (Prentice Hall, Inc., New Jersey, 2001)
39. N.M. Cann, A.J. Thakkar, J. Elec. Spec. **123**, 143 (2002)
40. M. Glass-Maujean, H. Schmoranzer, J. Phys. B **38**, 1093 (2005)
41. A.U. Hazi, K. Wiemers, J. Chem. Phys. **66**, 596 (1977)